

Atmospheric corrosion of mild steel^(*)

M. Morcillo*, D. de la Fuente*, I. Díaz* y H. Cano*

Abstract

The atmospheric corrosion of mild steel is an extensive topic that has been studied by many authors in different regions throughout the world. This compilation paper incorporates relevant publications on the subject, in particular about the nature of atmospheric corrosion products, mechanisms of atmospheric corrosion and kinetics of the atmospheric corrosion process, paying special attention to two matters upon which relatively less information has been published: a) the morphology of steel corrosion products and corrosion product layers; and b) long-term atmospheric corrosion (>10 years).

Keywords

Atmospheric corrosion; Mild steel; Long-term; Morphology; Review.

Corrosión atmosférica del acero suave

Resumen

La corrosión atmosférica del acero suave es un tema de gran amplitud que ha sido tratado por muchos autores en numerosas regiones del mundo. Este artículo de compilación incorpora publicaciones relevantes sobre esta temática, en particular sobre la naturaleza de los productos de corrosión atmosférica, mecanismos y cinética de los procesos de corrosión atmosférica, prestando una atención especial a dos aspectos sobre los que la información publicada ha sido menos abundante: a) morfología de los productos de corrosión del acero y capas de productos de corrosión, y b) corrosión atmosférica a larga duración (> 10 años).

Palabras clave

Corrosión atmosférica; Acero suave; Larga duración; Morfología; Revisión.

1. INTRODUCTION

Steel is used to make a wide range of equipment and metallic structures due to its low cost and good mechanical strength. Much of the steel that is manufactured is exposed to outdoor conditions, often in highly polluted atmospheres where corrosion is considerably more severe than in clean rural environments.

The atmospheric corrosion of mild steel is an extensive topic that has been studied by many authors, who have proposed different mechanisms and techniques for studying the phenomena involved and have reported exposure results in different regions throughout the world^[1-3]. Useful contributions have been performed by a number of researchers^[4-8], the most recent dating from the year 2000.

Atmospheric corrosion is a major problem for the application of engineering metals in many types of service. As a result there is an ongoing effort to

understand this phenomenon and develop standards that can be used to predict the severity of corrosion processes in service conditions^[9].

A great deal of information is available on the atmospheric corrosion of mild steel in the short and mid term. Information on long-term exposure (10 - 20 years) is much less abundant, and no consistent data is available for exposure times over 50 years^[10].

Considerable effort has been dedicated to identifying corrosion products and quantifying the effect of corrosion in terms of mass loss, and a number of models have been developed to describe the influence of various environmental parameters on the corrosion rate; particularly the sulphur dioxide and chloride concentration^[11]. However, an aspect that has been relatively less studied and reported is the morphology of the corrosion products that grow on steel surfaces in the form of thin or thick films.

^(*) Trabajo recibido el día 09 de mayo de 2011 y aceptado en su forma final el día 04 de agosto de 2011.

* Dept. Surface Engineering, Corrosion and Durability. National Centre for Metallurgical Research (CENIM, CSIC). Avda. Gregorio del Amo, 8. 28040-Madrid.

This review paper has identified some relevant publications on the subject, in particular about the nature of the corrosion products, mechanisms of atmospheric corrosion and kinetics of the atmospheric corrosion process, paying special attention to two matters upon which relatively less information has been published: a) the morphology of steel corrosion products and corrosion product layers; and b) long-term atmospheric corrosion (>10 years).

2. ATMOSPHERIC CORROSION PRODUCTS

Atmospheric corrosion products of iron and its alloys, referred to as “rust”, comprise various types of oxides, hydrated oxides, oxyhydroxides and miscellaneous crystalline and amorphous substances that form as a result of the reaction between materials and their environment. Such substances may originate from the substrate itself (endogenous products) or from the atmosphere (exogenous products).

The proportion in which each type of component occurs depends on the composition of the iron material and the environment to which it is exposed, as well as the intensity of and changes in meteorological factors, such as wind, temperature and rainfall, pollution conditions (natural or anthropogenic), etc. The exposure time is also highly influential.

2.1. Nature of atmospheric corrosion products

Table I lists the corrosion products found most frequently in the layers formed on mild steel exposed to the atmosphere. A group of Fe(II/III) hydroxy salts, known as green rusts because of their green-blue-greyish colour, are also often detected among atmospheric corrosion products on steel, and it is habitual to find non-crystalline (amorphous) and non-stoichiometric phases in iron corrosion product layers^[12 y 13].

In addition to the above compounds, iron can also form a number of different substances and be found in other minerals, some of which contain sulphur and can play a significant role in corrosion in urban and industrial atmospheres. Such compounds include iron(II) sulphur heptahydrate (melanterite), tetrahydrate (rozenite) or monohydrate; and iron(III) sulphate or Fe(SO₄)₃

Table I. Chemical compounds found in rust layers

Tabla I. Compuestos químicos encontrados en las capas de herrumbre

Name	Composition
Oxides	
Hematite	$\alpha\text{-Fe}_2\text{O}_3$
Maghemite	$\gamma\text{-Fe}_2\text{O}_3$
Magnetite	Fe_3O_4
Ferrihydrite	$\text{Fe}_5\text{HO}_8 \cdot 4\text{H}_2\text{O}$
Hydroxides	
Ferrous hydroxide	$\text{Fe}(\text{OH})_2$
Ferric hydroxide	$\text{Fe}(\text{OH})_3$
Goethite	$\alpha\text{-FeOOH}$
Akaganeite	$\beta\text{-FeOOH}$
Lepidocrocite	$\gamma\text{-FeOOH}$
Feroxyhyte	$\delta\text{-FeOOH}$
Others	
Ferrous chloride	FeCl_2
Ferric chloride	FeCl_3
Ferrous sulphate	FeSO_4
Ferric sulphate	$\text{Fe}_2(\text{SO}_4)_3$

hydrated to a variable extent. In corrosion in marine atmospheres, chloride-containing compounds such as iron(II) chloride or FeCl₂ (lawrencite), iron(II) chloride tetrahydrate or FeCl₂·4H₂O, and iron(III) chloride hexahydrate or FeCl₃·6H₂O can play an active role^[12].

Table II shows the water solubility of different iron compounds that usually form as a consequence of atmospheric corrosion^[14 y 15]. The most easily detected compounds are obviously the most insoluble, and therefore found in high concentrations. In contrast, iron chlorides and sulphates, which are soluble, are easily leached from the corrosion product layer by the action of rainwater, and their low residual concentration in the corrosion product layer makes them hard to detect.

2.2. Dependence on environmental conditions

The composition of the rust layer depends on the conditions in the surface electrolyte and thus varies according to the type of atmosphere. Fe(OH)₂ may form in neutral to basic solutions. In atmospheres

Table II. Solubilities in cold water of iron chemical compounds^[14 y 15]*Table II. Solubilidad en agua fría de compuestos químicos del hierro^[14 y 15]*

	Species	Solubility in cold water (g/100 cm ³)
Oxides	FeO	i.
	Fe ₂ O ₃	i.
	Fe ₂ O ₃ · x H ₂ O	i.
	Fe ₃ O ₄	i.
Hydroxides	Fe(OH) ₂	0.00015
	Fe(OH) ₃	i. [21]
Chlorides	FeCl ₂	64.4
	FeCl ₂ · 4H ₂ O	160.1
	FeCl ₃	74.4
	FeCl ₃ · 5/2H ₂ O	v. s.
	FeCl ₃ · 6H ₂ O	91.9
Sulphates	FeSO ₄ · H ₂ O	sl. s.
	Fe ₂ (SO ₄) ₃	sl. s.
	FeSO ₄ · 7H ₂ O	15.65
	FeSO ₄ · 5H ₂ O	s.
	Fe ₂ (SO ₄) ₃ · 9H ₂ O	440
Sulfides	FeS ₂	0.00049
	FeS	0.00062
	Fe ₂ S ₃	sl. d.
Carbonates	FeCO ₃	0.0067
	FeCO ₃ · H ₂ O	sl. s

i. = insoluble; s.= soluble; v.s. = very soluble; sl. s. = slightly soluble; sl. d.= slight decomposition.

polluted by SO₂, however, the surface electrolyte is usually mildly acidic and Fe(OH)₂ does not precipitate^[6].

Hiller^[16] considers γ-FeOOH to be the primary crystalline corrosion product. In mildly acidic solutions γ-FeOOH is transformed into α-FeOOH in a process that is dependent on the sulphate concentration and the temperature. α-FeOOH seems to be the most stable modification of ferric oxide hydroxides. The solubility of α-FeOOH is approximately 10⁵ times lower than that of γ-FeOOH^[17]. In a study performed by Almeida *et al.*^[18], involving one year of exposure in 19 unpolluted rural atmospheres in Ibero-America, X-Ray diffraction (XRD) analysis detected no crystalline phase at 4 sites (due to the low amount of corrosion products), only lepidocrocite at 6 sites,

and both lepidocrocite and goethite at the remaining 9 sites.

In marine atmospheres, where the surface electrolyte contains chlorides, β-FeOOH is found^[19]. The formation of detectable amounts of β-FeOOH on freely exposed steel surfaces seems to require high yearly average chloride deposition rates. However on rain-protected steel surfaces, β-FeOOH was found to be abundant in rust also when the chloride deposition rate was as low as 40 mg/m²/day^[20].

Magnetite is also formed as one of the main constituents. Magnetite may form by oxidation of Fe(OH)₂ or intermediate ferrous-ferric species such as green rust^[21]. It may also be formed by reduction of FeOOH in the presence of a limited oxygen supply^[22] according to



Magnetite is usually detected in the inner part of rust adhering to the steel surface of specimens that have been subjected to prolonged exposure, where oxygen depletion may occur^[21 y 22].

In industrial and urban sites a common feature is the presence of γ -FeOOH, α -FeOOH and Fe_3O_4 . Reflection lines corresponding to hydrated maghemite ($\gamma\text{-Fe}_2\text{O}_3\cdot\text{H}_2\text{O}$) have also been detected^[23]. The XRD diffraction patterns for these two oxides, magnetite and maghemite, are very similar and it is difficult to determine whether a mixture or just one compound is present.

Reported rust compositions vary widely as a result of differences in exposure conditions, identification techniques and data interpretation^[12]. Although there is general agreement about the presence of lepidocrocite and goethite in the rust composition, other authors assign prevalence to amorphous ferric oxyhydroxide^[24] or ferrosulphate^[25].

A number of authors mention magnetite as a second-order constituent^[24 y 26], most often in rust developed in marine atmospheres. When magnetite forms it is usually near the metal substrate, where the lower oxygen availability favours its development^[27 y 28].

Akaganeite is a typical component of rust developed in marine atmospheres. As shown by Keller^[19], it can contain up to 6 % chloride and be formed at an early corrosion stage in chloride-containing solutions by hydrolysis of FeCl_3 or oxidation of FeCl_2 in the presence of iron. Nomura, *et al.*^[29] suggested an alternative formation pathway, where OH^- and Cl^- react concurrently with Fe^{3+} complexes to yield lepidocrocite and akaganeite, respectively. On contacting the steel surface, akaganeite is gradually transformed into magnetite, which may be the origin of discrepancies in the relative significance of these two constituents^[30].

Maghemite and hematite have also been found on steel surfaces exposed in different types of atmospheres^[31].

Water-soluble compounds such as FeCl_3 and FeSO_4 , though expected to be present, are often not detected by Energy Dispersive Spectroscopy (EDS). This may be because the amounts in question are so small that they are below the detection limit of the instrument, or because they are obscured by the complexity of the oxide scale after prolonged exposure. Water-soluble compounds have been analysed by Oesch and Heimgartner^[32] in Switzerland using ion chromatography with aqueous extracts from plate specimens. Pollution of the surfaces by ionic species varied greatly between the different test sites. As expected, the highest sulphate and chloride

concentrations were found on sheltered specimens. The values obtained only serve to give an idea of the situation at the time when the specimens were withdrawn, since they tend to be strongly dependent on deposition and precipitation conditions in the preceding days and weeks. In a study conducted by Flores and Morcillo^[33 y 34] on a set of unalloyed low-carbon steel specimens which had been exposed outdoors in 64 different atmospheres of the Iberoamerican region, covering a broad spectrum of atmospheric conditions, the following conclusions were found:

- a) Non-adherent rust contents were lower than 34 % of the total rust and frequently, much lower.
- b) Both, soluble chlorides and soluble sulphates, tend to accumulate in the adherent rust layer. This accumulation of contaminants can be ascribed to various causes, including the anionic migration mechanism proposed by Evans^[59] and, among others, the washing by rain-water of the outer sublayer of corrosion products layer.
- c) A clear dependence of the soluble chloride content in the rust with the atmospheric salinity was been found. Such correlation was not as clear in the case of soluble sulphates in the rust and SO_2 content in the atmosphere.

2.3. Morphology

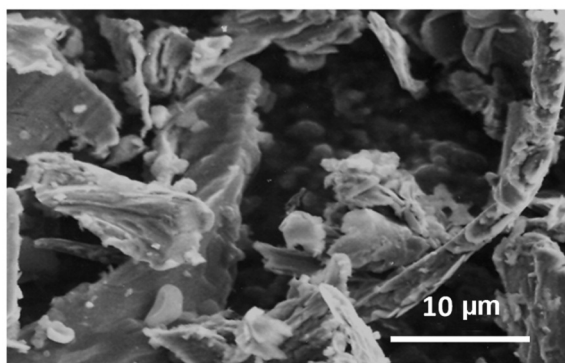
An aspect that has been relatively less studied is the morphology of the corrosion products that grow on the steel surface in the form of thin or thick films. According to Cindra Fonseca, *et al.*^[35], it is strange that although Scanning Electron Microscope (SEM) is very useful to show morphology, and is widely used in materials science, it has not until relatively recently become a common technique in atmospheric corrosion studies.

For most iron corrosion products there is more than one possible preparatory method, and the crystal morphology depends on these preparatory conditions^[13], so a wide range of crystal morphologies and crystal sizes are displayed by most iron corrosion products, a fact that has given rise to confusion on the part of many researchers when assigning a morphology to a certain corrosion product.

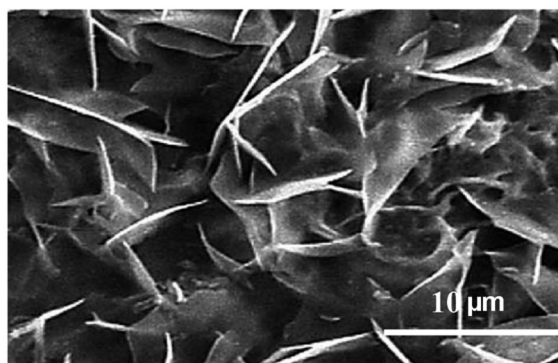
The surface morphology can vary considerably between different exposure sites. The morphology of the oxide layer formed on mild steels has been observed by a number of authors^[25, 31, 36-42]. The phases most frequently found present typical

structures (Fig. 1), for instance: lepidocrocite appears as small crystalline globules (sandy crystals) or as fine plates (flowery structures); goethite

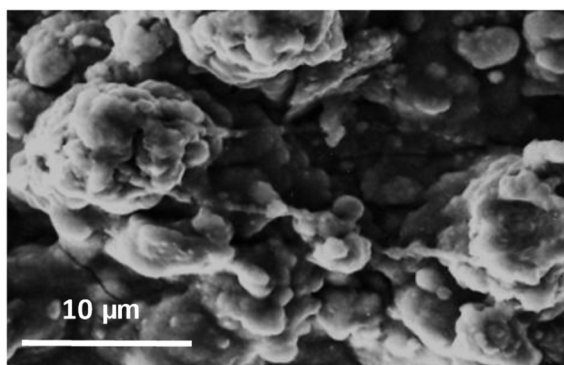
appears as globular structures known as cotton balls (semi-crystalline goethite) or even as acicular structures (crystalline goethite); feroxyhyte shows



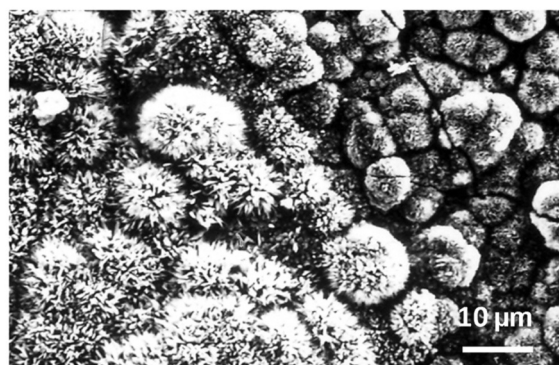
(A)



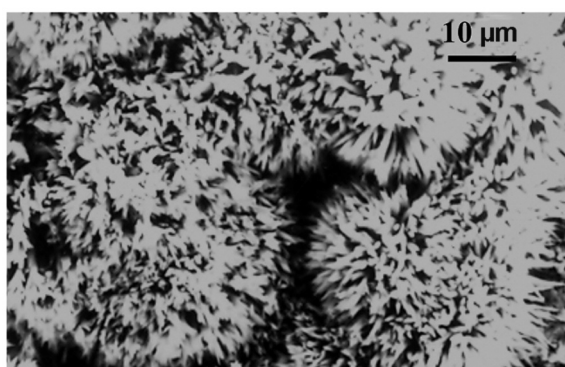
(B)



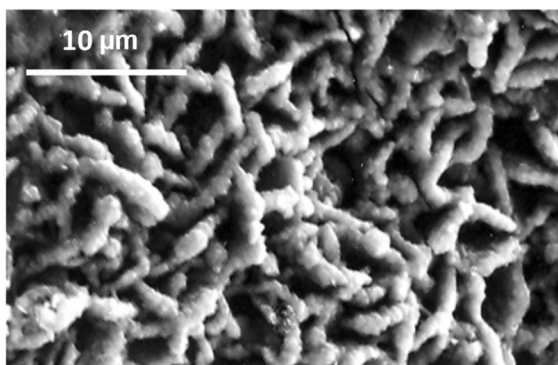
(C)



(D)



(E)



(F)

Figure 1. SEM micrographs showing: fine plates (“flowery” structures) (A-B) typical of lepidocrocite, globular (cotton balls) (C) and fine whiskers (D) typical of goethite, and “cotton balls” (E) and cigar-shaped crystals (F) typical of akaganeite^[37-41].

Figura 1. Micrografías obtenidas por SEM que muestran distintas morfologías de los productos de corrosión del acero: finas láminas (estructuras “floridas”), típicas de lepidocrocita (A-B); estructuras globulares (“bolas de algodón”) (C) y finas agujas (D), típicas de goetita, y “bolas de algodón” (E) y cristales de forma “tubular” (F), típicas de akaganeita^[37-41].

a distorted plate-like morphology^[42] and akaganeite appears with cotton ball and rosette morphologies or cigar-shaped crystals^[42 y 43]; this last structure is not commonly referred to in atmospheric corrosion studies of steel^[36 y 43]. Asami and Kikuchi^[44] and Kamimura, *et al.*^[45] associate this compound to belt-like-shaped crystallites with a fibre (hollandite) structure. Magnetite comes out as dark flat regions, with circular discs that are more difficult to find^[45].

3. MECHANISMS OF ATMOSPHERIC CORROSION

3.1. From early stages to ¿steady-state conditions? [7]

When the metal ion dissolves into the liquid layer it can coordinate with counterions that are present. This ion-pairing process depends on the nature of the metal ion and the counter ion.

When the ion-pair concentration in the liquid layer eventually reaches supersaturation, the ion pairs will precipitate into a solid phase. This precipitation process is complex, and the precipitated species may pass through a colloidal state before reaching the solid state. The nucleation of precipitated species is facilitated by the heterogeneous nature of the substrate surface, in particular by solid-state defects of various kinds, which can act as nucleation sites.

With prolonged exposure, the number and size of precipitated nuclei increases by growing and coalescence until eventually they completely cover the metal surface. The precipitates at this stage are normally referred to as “corrosion products” and play a very important role in the behaviour of any material in a given environment.

When the thin layer of corrosion products has grown to cover the whole surface, further growth requires reactive species from the liquid layer to be transported inwards, metal ions to be transported outwards, or both transport processes to occur simultaneously.

In addition to the transport of ions, the transport of electrons from anodic to cathodic reaction sites on the surface has to be considered. This transport is a necessary process so that electrons produced in the anodic reaction can be consumed in the cathodic reaction.

Due to the ready availability of oxygen in thin liquid films, it is generally believed that the transport of oxygen from the atmosphere to the cathodic site is not a rate-limiting step. Exceptions occur if the

liquid layer exceeds a thickness of several tenths of a micron, in which case oxygen transport may become rate-limiting, or if the corrosion product film develops so as to hinder electron or oxygen transport.

The long-term growth of corrosion products is highly dependent on the actual exposure conditions. Continuously repeated cycles of dissolution, coordination and precipitation cause the corrosion product layer to age by changing its chemical composition, microstructure, crystallinity, thickness and other properties.

When the corrosion products eventually acquire characteristics that no longer change with time, the corroding material becomes characterised by a constant corrosion rate. This means that the corrosion product finally reaches a constant thickness, with a certain amount of material corroding away per unit of time and the same amount of material running off the corrosion products during that time. The time needed to reach steady-state atmospheric corrosion conditions may be several years or even decades.

According to Kucera and Mattsson^[6], two general stages may be distinguished in the atmospheric corrosion of iron: initiation and propagation.

Initiation

In a dry, clean atmosphere the steel surface becomes coated with a 20-50 Å thick oxide film that practically prevents further oxidation. This oxide film consists of an inner layer of Fe₃O₄ and an outer layer of polycrystalline Fe₂O₃.

The initiation of corrosion on a clean metal surface in non-polluted atmospheres is a very slow process, even in atmospheres saturated with water vapour. In this case, initiation may occur at surface inclusions such as MnS, which dissolve when the surface becomes wet^[46 y 47]. Another important factor for the initiation of corrosion is the presence of deposited solid particles on the surface^[48].

Propagation

During the initiation period, anodic spots surrounded by cathodic areas are formed. In the presence of the necessary layers of water on the metal surface structure, conditions are created for propagation of the corrosion process.

3.2. Rust formation mechanisms

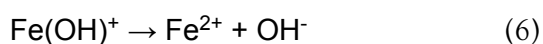
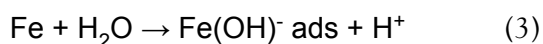
A comprehensive discussion of this topic entails, considering the models developed to account for the atmospheric corrosion of steel, including Schikkor's "acid regeneration cycle"^[49], the electrochemical theory of Evans^[50 y 51] and its refined version by Stratmann^[52-56].

The following equations may in principle describe the reactions taking place in the corrosion cells^[6].

At the anode

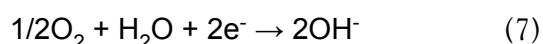


The mechanism of iron dissolution may be described as follows according to Heusler^[57] and Bockris *et al.*^[58]:



At the cathode

The main cathodic reaction is considered to be reduction of oxygen dissolved in the electrolyte film:



This process causes a local increase in pH at the cathodes and promotes the precipitation of corrosion products at some distance from the anodes.

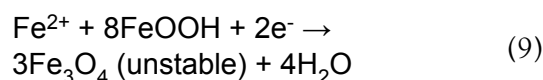
As soon as ferric corrosion products have been formed, another cathodic process may take place:



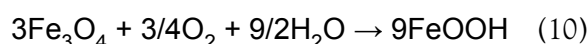
3.2.1. Evans' model

Evans^[50, 51 y 59] developed an electrochemical model to explain the observed influence of changing wetness on the atmospheric corrosion of iron. He postulated that in periods of high water content within the porous structure of the rust, the anodic dissolution of

iron is balanced by the cathodic reduction of Fe(III) oxides in the rust layer:



Later, after partial drying of the pore structure, magnetite is reoxidised by oxygen that now has free access through the pores due to gas diffusion:



After wetting, the cycle of FeOOH reduction and Fe₃O₄ oxidation can start again. This mechanism rests on lepidocrocite, which is supposed to be the only reactive phase in the corrosion layer. However, Nishimura *et al.*^[60] studying steels covered with a rust layer containing β-FeOOH, electrochemically showed that β-FeOOH is also easily reducible and can promote corrosion in environments with chlorides.

Several papers^[61-63] concerned with rust reduction have subsequently been reported. The relevant role of lepidocrocite in the corrosion process is shown in the electrochemical study by Antony *et al.*^[64], which concludes that a galvanic coupling between γ-FeOOH reduction and iron oxidation is possible. A number of authors^[21, 66 y 67] have shown that atmospherically formed rust layers can easily be reduced, observing the formation of Fe₃O₄ usually from γ-FeOOH.

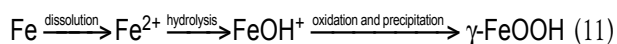
3.2.2. Misawa's model

The consensus in the early 1970's was that the main products of rust formed on mild and low alloy steels in atmospheric corrosion were α-FeOOH, γ-FeOOH, Fe₃O₄ and X-ray amorphous matter. β-FeOOH is often found in the rust layer on steels exposed in marine atmospheres. However, the mechanism of the formation of α-FeOOH, γ-FeOOH and amorphous matter in atmospheric rusting was not completely understood. In particular, the composition of amorphous matter remains undetermined.

Misawa *et al.*^[24] characterised X-ray amorphous matter as amorphous ferric oxyhydroxide FeO_x(OH)_{3-2x} by XRD and IRS, formulating the following mechanism of atmospheric rusting:

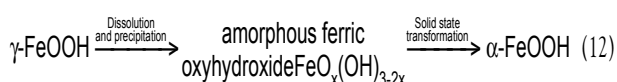
(a) Rusting starts with the formation of γ-FeOOH in a neutral to slightly acidic solution. In the first

stage of rusting the aerial oxidation of ferrous ions, dissolved from the steel into a slightly acidic thin water layer formed by rain on the steel surface, leads to the precipitation of γ -FeOOH. Fine weather accelerates the precipitation and crystallisation of γ -FeOOH by drying.



(b) The γ -FeOOH content is higher in inner rust layers than in outer layers, which contain large amounts of amorphous ferric oxyhydroxide and α -FeOOH. This suggests that γ -FeOOH is formed on the steel surface and transformed to amorphous ferric oxyhydroxide and α -FeOOH from the outer part upon atmospheric rusting as follows:

It is known that fresh rain dissolving impurities including SO_2 in the atmosphere often shows a low pH value, such as pH 4. Such a low pH water layer dissolves γ -FeOOH and results in the precipitation of amorphous ferric oxyhydroxide with drying. The amorphous ferric oxyhydroxide transforms to α -FeOOH by deprotonation using hydroxyl ions provided by the rain.

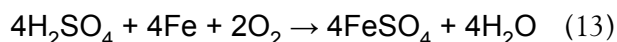


The wet-dry cycle accelerates these rusting process, especially precipitation and transformation with deprotonation and dehydration.

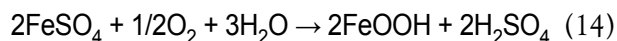
Misawa notes that the main constituent of rust in a rural (unpolluted) atmosphere is γ -FeOOH, while in an atmosphere containing SO_2 a large amount of α -FeOOH is detected. This is in agreement with the results of a study performed in a large number of rural atmospheres ($<3 \text{ mg Cl/m}^2/\text{day}$ and $\leq 10 \text{ mg SO}_2/\text{m}^2/\text{day}$) in Ibero-America^[18], although with different time of wetness (TOW). In the first year of exposure a considerable variety of corrosion rates was obtained, from $1.4 \mu\text{m}$ in Cuzco (Peru) to 28.1 in La Plata (Argentina). The corrosion products identified were lepidocrocite (always) and goethite (only when corrosion rates were high and corresponded to rural atmospheres with the highest SO_2 levels).

3.2.3. Schikorr's model

Schikorr^[49] proposed a theory of atmospheric corrosion of steel based on the "acid regeneration cycle". Sulphuric acid, formed by oxidation of SO_2 absorbed in the rust layer, attacks the steel according to the overall reaction:



Sulphuric acid is then re-formed by oxidative hydrolysis:



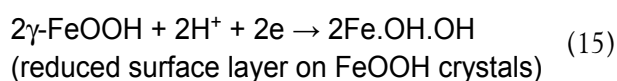
Although Schikorr's theory does not explain the detailed mechanism of the corrosion process, it shows oxidative hydrolysis to be very important in the steel atmospheric corrosion process^[68]. It should, however, be mentioned that according to Evans and Taylor^[51] the oxidative hydrolysis of FeSO_4 is very slow and should only affect corrosion during the initiation stage.

3.2.4. Stratmann's model

Stratmann *et al.*^[69], in an electrochemical study of phase transitions in rust layers, experimentally showed that the oxidation of Fe_3O_4 to γ -FeOOH (reaction (10)), as proposed by Evans^[50, 51 y 59], was not possible. Thus, in 1987 Stratmann^[69] proposed dividing the atmospheric corrosion mechanism of pure iron into the following three stages:

Stage 1: wetting of the dry surface

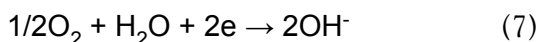
As proposed by Evans^[50 y 59] and Evans and Taylor^[51], a corrosion cell starts where the anodic dissolution of iron is balanced by the cathodic reduction of Fe(III) in the rust layer:



During this stage the cathodic O_2 reduction reaction is very slow compared to anodic iron dissolution. The metal dissolution rate is high, but the amount of dissolved iron is restricted to the amount of reducible FeOOH in the rust layer^[52].

Stage 2: wet surface

Once the reducible FeOOH has been used up, the O_2 reduction reaction becomes the cathodic reaction:



The metal dissolution rate is determined by the diffusion limited current density of the O_2 reduction reaction on the pore surfaces. Because the pores in the rust layer are filled with electrolyte, the corrosion rate is quite slow during stage 2, as the diffusion rate is lower in the electrolyte than in the gas phase.

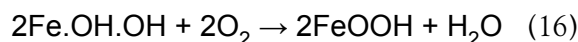
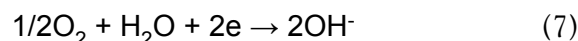
Electrochemical studies by Stratmann and Müller^[54] showed for the first time that oxygen is reduced within the oxide scale and not at the metal/electrolyte interface. This implies that the electronic structure of the oxides will strongly influence the reduction of oxygen and therefore also the corrosion rate. The atmospheric corrosion rate is determined for thin films by the electronic properties of the rust layer, and the corrosion rate immediately decreases as the oxides are reoxidised^[55].

Stage 3: drying-out of the surface

During drying out, the rate of the diffusion limited O_2 reduction reaction is extremely fast due to

thinning of the electrolyte film on the inner surface of the rust layer. Accordingly, the corrosion rate is very high, O_2 reduction again being the cathodic reaction.

In addition to this, O_2 can reoxidise the reduced Fe^{2+} formed in stage 1:



As a consequence of the high corrosion rate, stage 3 seems to dominate the metal loss during the whole wet-dry cycle.

In the third stage, the reduced layer of $\gamma\text{-FeOOH}$ and the other ferrous species are reoxidised by oxygen, leading to the formation of goethite and the regeneration of lepidocrocite. The electrolyte film is used up, stopping the corrosion process completely. It is during this final stage that the rust layer composition changes, leading to a different intensity in the corrosion process for the next wet-dry cycle (Fig. 2).

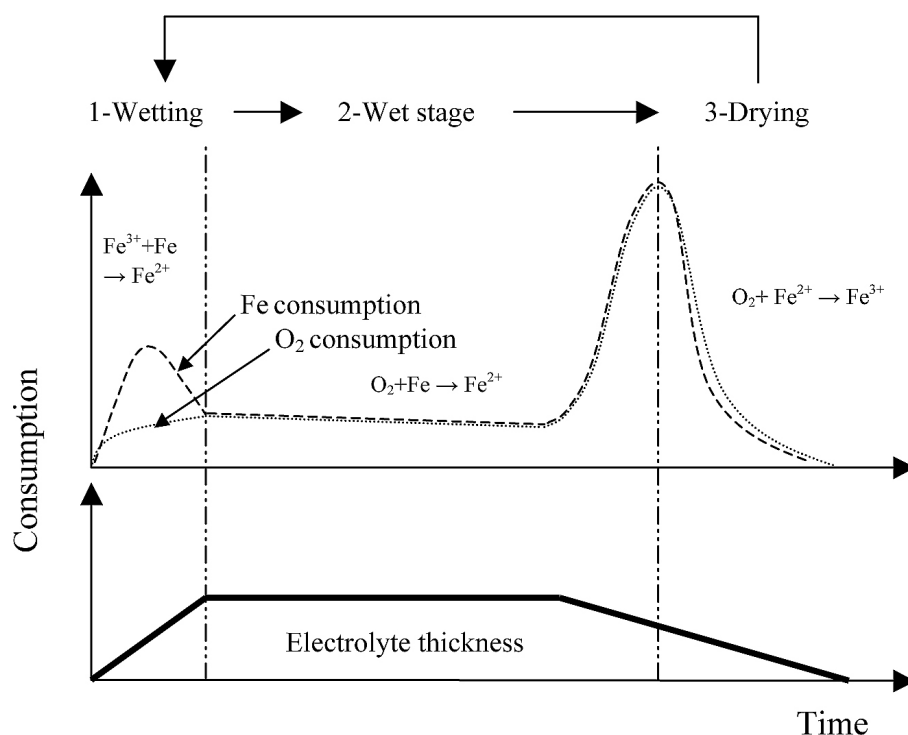


Figure 2. Rusting mechanism according to Stratmann^[70]. Wet-dry cycle.

Figura 2. Mecanismo de formación de herrumbre según Stratmann^[70]. Ciclo de humectación-secado.

3.3. Corrosion of steel in polluted atmospheres

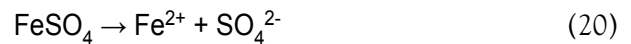
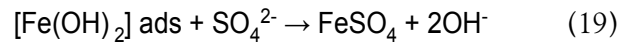
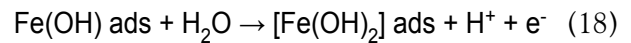
3.3.1. Atmospheres polluted with SO₂

Numerous researchers have carried out laboratory studies to reveal the mechanisms by which SO₂ acts in the atmospheric corrosion of metals, and in particular its combined effect with humidity. Vernon^[48] was the first to show the important accelerating effect of SO₂, and the fact that there is no appreciable corrosion without the simultaneous intervention of pollutants and humidity; even the highest SO₂ concentrations have no effect on steel at ambient temperature in atmospheres without water vapour.

The atmospheric corrosion process is stimulated by SO₂, which is adsorbed and oxidised in the rust layer to SO₄²⁻. In the corrosion cells, sulphate accumulates at the anodes and thus creates so-called sulphate nests in the rust, which were first described by Schwarz^[71]. In the initial stage the surface is covered by a great number of small sulphate nests. With increasing exposure times the nests grow larger and their number per unit area decreases.

When the surface becomes wetted by rain, dew or moisture adsorption, the sulphate nests in combination with the surrounding area form corrosion cells (Fig. 3). The electrolyte is mostly very concentrated and has a low water activity. Anodes are located inside the sulphate nests.

In sulphate-containing solutions the anodic dissolution proceeds according to a mechanism proposed by Florianovitch *et al.*^[73]:



The pH-regulating effect of FeSO₄ will result in maintaining a relatively low pH at the anodic sites and thus preventing precipitation of iron hydroxides directly on the metal surface. This creates favourable conditions for corrosion in the active state, as the sulphate accelerates the anodic dissolution of iron. Tanner^[74] identified crystalline iron(II) sulphate at the steel/rust interface as tetrahydrate FeSO₄·4H₂O. Thus a reservoir of soluble sulphates exists within the sulphate nests, contributing to their high stability.

The sulphate nest becomes enclosed within a semipermeable membrane of hydroxide formed through oxidative hydrolysis of the iron ions (Fig. 3). The electrical current in the corrosion cell causes migration of SO₄²⁻ ions into the nest. This will stabilise the existence of the nest.

Hydrolysis of the ferrous sulphate formed in these nests controls their propagation. The osmotic pressure can cause them to burst, thus increasing

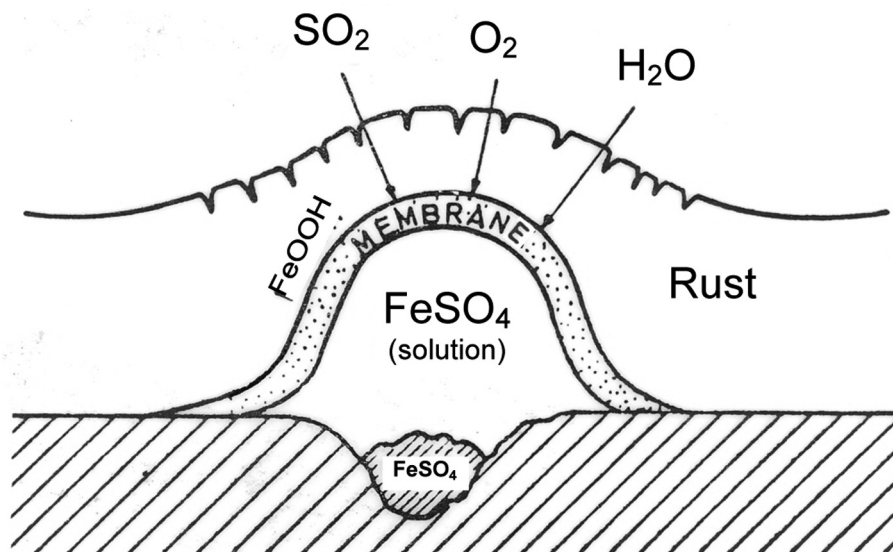


Figure 3. Schematic representation of a sulphate nest^[72].

Figura 3. Representación esquemática de un nido de sulfato^[72].

the corrosion rate. The nests are covered by a membrane containing FeOOH. The higher the amorphous FeOOH content, the greater the stability of this membrane and the more unlikely it is to burst due to the effect of osmotic pressure and the repeated wetting and drying of the rust layer.

Attention is drawn to the important research carried out by Ross and Calaghan^[75] in relation with sulphate nests. SEM has allowed an insight into the phenomenon of seasonal migration of sulphur, as a sulphate, in the rust layer of a carbon steel. When steel is exposed to atmospheres polluted with SO₂, sulphur accumulates during the winter in a band at the metal-oxide interface. With the arrival of summer, the sulphur becomes concentrated in nests, and is then diffused homogeneously throughout the thickness of the rust layer.

3.3.2. Atmospheres polluted with chlorides

In atmospheres polluted with chlorides the corrosion of carbon steel proceeds in local cells which resemble the sulphate nests mentioned above^[76]. They may arise around chloride particles deposited on the surface, where the concentrated chloride solution locally destroys the FeOOH passivating film. In the anodic areas so formed the chlorides are concentrated by migration, while the rust-coated surrounding area acts as a cathode. However, unlike in the case

of atmospheres polluted with SO₂, nests are not formed.

The osmotic pressure of ferrous chloride or sodium chloride does not influence corrosive activity, which is determined by other causes such as the ability of ferrous and ferric chlorides to form complexes. Oxidant hydrolysis does not give rise to FeOOH but to the complex nFeOOH.FeCl₃, or a solution of FeCl₃ in FeOH in gel form^[72]. No amorphous oxide/hydroxide membrane is formed (Fig. 4). It is fairly common to find iron chlorides among the iron corrosion products, which tend to accumulate at the steel/rust interface by migration (Fig. 5).

In marine atmospheres, in addition to γ -FeOOH and α -FeOOH, akaganeite and magnetite could be also formed. The latter species tends to be concentrated in the innermost zones of the rust layer, where it is hardest for oxygen to reach. In contrast, akaganeite forms in the most superficial zones of the rust layer^[44].

3.3.3. Atmospheres polluted by SO₂ and Cl⁻ (coastal-industrial)

Sea chlorides from natural airborne salinity together with SO₂ play an important role in determining the magnitude of atmospheric steel corrosion. However, the scientific literature contains relatively little information on atmospheric corrosion in this type of mixed atmospheres.

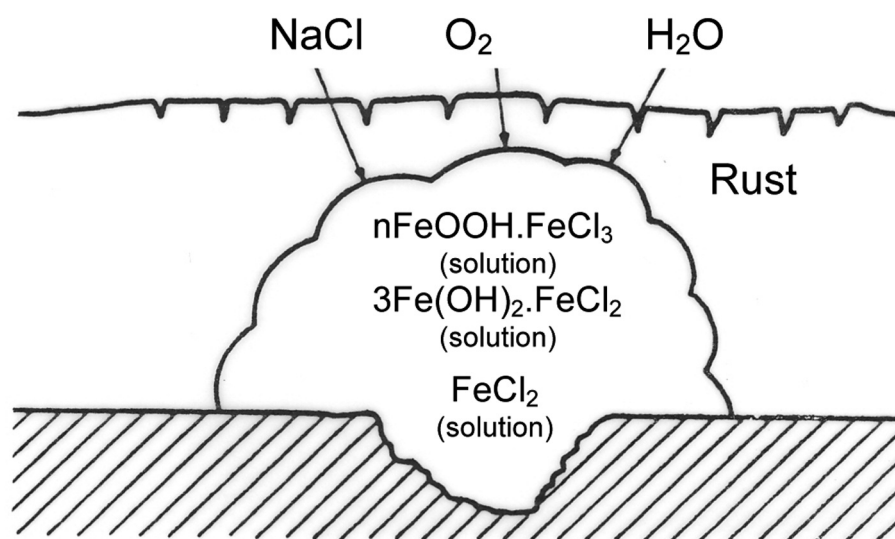


Figure 4. Schematic representation of a chloride agglomerate^[72].

Figura 4. Representación esquemática de un aglomerado de cloruro^[72].

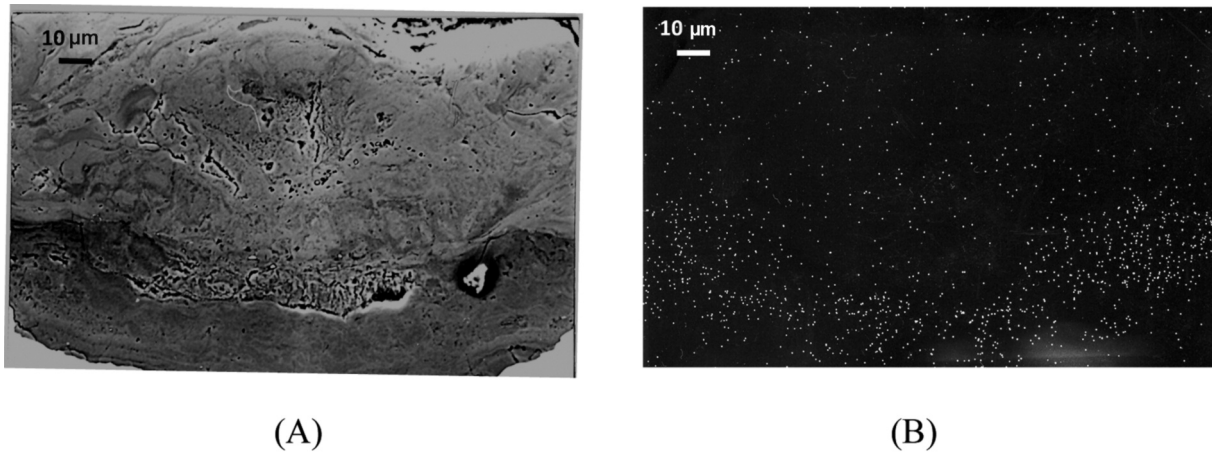


Figure 5. A: Cross section BSE/SEM micrograph of the rust layer formed in a marine atmosphere showing a region rich in chlorides (dark area). B: X-ray map of chloride^[36].

Figura 5. A: Observación microscópica mediante BSE/SEM de la sección transversal de una capa de herrumbre formada en una atmósfera marina, que muestra una región rica en cloruros (zona oscura). B: Mapa de rayos X del Cl^[36].

In a study carried out by Allam *et al.*^[77] in an industrial environment near the west coast of the Arabian Gulf, attention is paid to the combined effect of sulphur dioxide and sodium chloride on atmospheric corrosion during the initial stages (12 months). The results indicated that atmospheric corrosion started with the formation of small blisters at discrete locations on the metal surface, presumably the anodic sites. The blister covers were very rich in iron chlorides and contained iron oxyhydroxides, oxides, sulphates and possibly hydroxide.

The formation of iron chlorides as major constituents in the blister covers indicated that chloride ions were more aggressive than sulphate ions during the initial stages of atmospheric corrosion. Further formation of iron chlorides depended on the supply of chloride ions to the metal-rust interface. As the blisters grow to form a thick continuous layer of corrosion products, the supply of chloride ions and subsequently the formation of iron chlorides will eventually dwindle, compared to the initial stages. In contrast, further formation of iron sulphates at the metal-rust interface takes place during extended exposure, initially via the acid regeneration mechanism and subsequently by the electrochemical mechanism. It is thus less dependent on the transport of fresh sulphate ions through the thickened rust layer from the surface electrolyte layer to the metal-rust interface.

The diversity of industrial environments, with the possible presence of other pollutants that may

influence the corrosion process, has given rise to several papers on the synergic effect of both pollutants (SO₂ and chlorides), while others speak of a competitive absorption effect^[78] Thus, Ericson^[79] speaks of a synergic effect of the combined influence of 1 μg SO₂/cm²/hour (1 ppm SO₂) and sodium chloride crystals on the sample surface in exposure at 90 % relative humidity. However, at 70 % relative humidity sulphur dioxide did not affect the corrosion of steel with sodium chloride particles on its surface.

Almeida *et al.*^[80], in a study carried out in a large number of corrosion stations with varying contents of the two pollutants, made the following observations:

(a) In atmospheres with low Cl⁻ pollution (3 < Cl⁻ ≤ 60 mg/m²/day) and low SO₂ pollution (10 < SO₂ ≤ 35 mg/m²/day) the atmospheres showed corrosivity categories C2-C3 according to ISO 9223^[81] and presented relatively compact and rounded structures characteristic of the presence of SO₂, especially composed of lepidocrocite and goethite.

(b) Higher Cl⁻ pollution (60 < Cl⁻ ≤ 300 mg/m²/day) of the atmosphere meant higher steel corrosion rates of to C3 to ≥ C5^[81]. The incorporation of chloride ions in the open steel corrosion product layer structures seems to have a detrimental effect on atmospheric corrosion resistance.

(c) A higher SO₂ concentration (35 < SO₂ ≤ 80 mg/m²/day) led to significant stabilisation of the steel corrosion layers with exposure time and consequently a significantly lower steel corrosion rate (C4)^[81].

4. LONG-TERM EXPOSURES

4.1. Nature of corrosion products

The nature of rust constituents is barely affected by exposure time; in fact, it seems that nearly the same species are always detected at a given site, however long the exposure. The time factor only alters the proportions of the constituents or, at most, determines the appearance or disappearance of intermediate or minor compounds.

It is interesting information to know what phases are present in rust according to the type of atmosphere where mild steel has been exposed for long time periods^[36].

Asami and Kikuchi^[44] analysed rust on mild steel exposed for 17 years in a rural atmosphere. XRD revealed α -FeOOH as the main constituent, along with γ -FeOOH and β -FeOOH. The origin of β -FeOOH was Cl⁻ from calcium chloride (rather than marine NaCl) used to melt snow on roads during the winter. Magnetite was not detected, because the X-ray incident angle was fixed at 10°, and the results obtained were just from the surface region of the rust layer. These results do not rule out the existence of magnetite underneath.

Dillmann *et al.*^[10], in ancient ferrous artefacts exposed for very long times (several hundred years) to atmospheres of low aggressivity (rural or semi-industrial, not marine), analysed the composition of rust layers using micro-X-ray diffraction under synchrotron radiation (μ XRD) and micro-Raman spectroscopy. μ XRD showed that α -FeOOH was present in greater proportions (inner layers) than γ -FeOOH (outer layers). The proportion of magnetite found was 10%, while β -FeOOH was less frequent, but it was obviously not possible to identify the amorphous phases. In contrast, micro-Raman spectroscopy detected a poorly crystallised maghemite phase and ferrihydrite. The identification of ferrihydrite was confirmed by X-ray absorption methods under synchrotron radiation^[82].

Kamimura *et al.*^[45] characterised rusts formed on a mild steel exposed for 15 years in an industrial environment using Mössbauer spectroscopy and XRD. They reported that the rust formed consisted of crystalline phases (α - and γ -FeOOH) and an amorphous-like phase, $\text{Fe}_{3-x}\text{O}_4$ (γ -Fe₂O₃) that exceeded 50 % of the total amount of rust. This amorphous phase was present both in the inner and the outer rust layer.

Oh and Cook^[83] analysed rust on mild steel exposed for 16 years in an industrial atmosphere using XRD, Raman spectroscopy and Mössbauer spectroscopy. XRD identified the crystalline phases

as α -FeOOH and γ -FeOOH, and Raman spectroscopy confirmed the presence of both and identified γ -Fe₂O₃ and Fe₃O₄, while Mössbauer allowed a finer characterisation detecting α -FeOOH (magnetic and superparamagnetic with different phase sizes), γ -FeOOH and γ -Fe₂O₃.

Cook^[84], with mild steel exposed for 16 years at rural and industrial sites, showed that a decrease in the amount of nanophase goethite was responsible for increased porosity and time-of-wetness on the steel surface. This in turn led to the formation of maghemite in the less-aerobic environment close to the steel.

Yamashita *et al.*^[85] reported the influence of airborne salt in marine atmospheres on the rust structure, pointing to an increase in the β -FeOOH content and rust particle size as the airborne salt level increased. Magnetite was also found, even when the atmospheric salinity was low.

Oh *et al.*^[83] analysed rusts formed on mild steel exposed for 16 years to a moderate marine atmosphere. Using XRD they found goethite, lepidocrocite, maghemite or magnetite, and akaganeite (possible). Raman spectroscopy ruled out the presence of akaganeite and revealed the existence of both maghemite (< 5 %) and magnetite (< 1 %). Finally, using Mössbauer spectroscopy they performed a finer identification, revealing and quantifying the presence of magnetic and superparamagnetic goethite (of different sizes) and superparamagnetic maghemite.

Asami and Kikuchi^[44] also analysed rusts formed on mild steel exposed for 17 years to a coastal industrial atmosphere. The distribution and abundance of α -FeOOH, β -FeOOH, γ -FeOOH, amorphous rust and magnetite in the rust layer were also investigated using transmission electron microscopy (TEM) and electron diffraction (ED). They found that the magnetite concentration was negatively correlated with the akaganeite concentration.

4.2. Morphology of corrosion layers

Recognition of the structure of the rust layer has not commonly been performed in atmospheric corrosion studies.

Rust structure characterisation has traditionally been done using techniques such as optical microscopy, polarised light microscopy, SEM, and electron probe microanalysis (EPMA). However, new techniques that have recently started to be used include TEM/ED and micro-Raman spectroscopy.

Backscattered electron imaging (BSE) in the SEM has successfully been used to study the microstructure of corrosion layers. Moreover, the sensitivity of the backscattered signal to small differences in the average atomic number makes it possible to know the distribution of sulphur and chloride compounds in the corrosion layers^[86].

Rust layers usually present considerable porosity, spallation and cracking. Cracked and non-protective oxide layers (open structure) allow the corrosive species easy access to the metallic substrate, and is the typical situation in atmospheres of high aggressivity. In contrast, compact oxide layers (closed structures) favour the protection of the metallic substrate. The greater the corrosivity of the atmosphere, the easier it is to find very open structures where flaking can occur. The higher the chloride deposition rate in marine atmospheres, the greater the degree of flaking observed, with loosely adherent flaky rust favouring rust film breakdown (detachment, spalling) and the initiation of fresh attack.

In atmospheric exposure, wetting and drying cycles influence the structure of the rust layer and its protective properties. Rust formed on steel freely exposed to rain shows a dense (less porous) and laminated structure, compared to the less protective powder-like grainy structure of rust formed on sheltered surfaces^[87] where diffusion to the steel/rust interface is less impeded.

The interior of rust layers exhibit a large number of pores (voids) and microcracks that make them highly defective and permeable to further attack. As time elapses, the number and size of defects may decrease due to compaction, agglomeration, etc. of the rust layer, thereby lowering the corrosion rate.

The use of complementary analytical techniques, such as X-ray micro diffraction (μ XRD), X-ray absorption under synchrotron radiation, Mössbauer spectroscopy, SEM/EDS, TEM/ED, Raman spectroscopy, etc., has allowed a more precise description of the structure of the corrosion product layer and therefore helped to a better understanding of the corrosion layers formed after exposure in air.

4.2.1. Stratification of the rust layer

There is controversy about the stratification of the rust layer in different sublayers^[12], as occurs in the case of weathering steels. Some authors, for example Suzuki *et al.*^[88] notes that the rust layer formed on unalloyed steel generally consists of two regions: an inner region, next to the steel/rust interface, often consisting primarily of dense amorphous FeOOH with some crystalline Fe₃O₄; and an outer region consisting of loose crystalline α -FeOOH and γ -FeOOH (Fig. 6(A)). However others, as Okada *et al.*^[89], report the inexistence of a dual-layer structure on mild steel exposed to atmospheric corrosion (Fig. 6 (B)).

Most researchers endorse the concept of a dual-nature rust layer with some or other predominant constituents, and in any case, the occurrence of a heavier, more adherent inner sublayer that affords protection and a weaker, more permeable outer sublayer, are supported for both mild steel and weathering steel.

Asami and Kikuchi^[44] and Dillmann *et al.*^[10] studied in detail the distribution of corrosion products and elements in the rust layer on mild steel, and

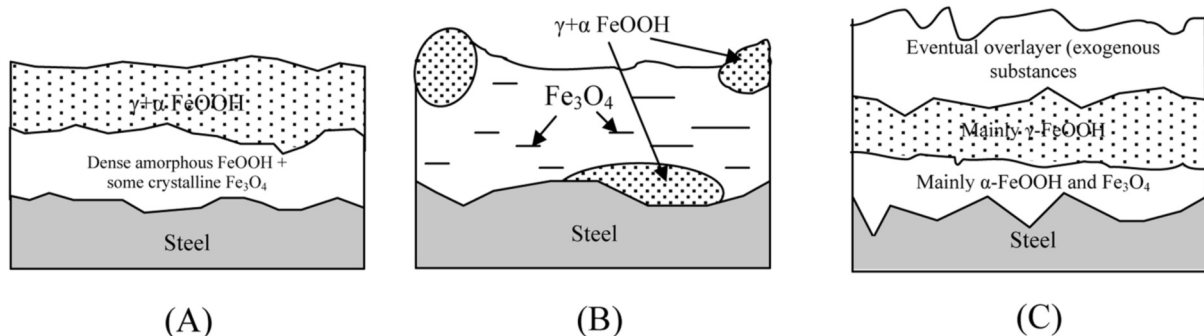


Figure 6. Controversy about the dual-nature of the rust layer, according to Suzuki *et al.*^[88] (A), Okada *et al.*^[89] (B), and Asami and Kikuchi^[44] (C).

Figura 6. Controversia acerca de la naturaleza dual de la capa de herrumbre según Suzuki *et al.*^[88] (A), Okada *et al.*^[89] (B), and Asami and Kikuchi^[44] (C).

reported that the rust layer often consists of three layers (Fig. 6 (C)): the inner layer, an outer layer and an outermost layer. This external sublayer can accumulate exogenous substances present in the atmosphere, such as chlorides, silica and alumina, originating from sea aerosols and atmospheric deposits of soils, sand, dust, etc.

4.2.2. Distribution of corrosion products inside the corrosion layers

Kamimura *et al.*^[45] characterised rusts formed on mild steel exposed for 15 years in an industrial environment using Mössbauer spectroscopy and XRD. They reported that the rust consisted of crystalline α -FeOOH, γ -FeOOH, and an amorphous-like phase, and that the amount of amorphous-like phase exceeded 50 % of the total rust. Mössbauer spectra indicated that the rust contained only α -FeOOH, γ -FeOOH and $\text{Fe}_{3-x}\text{O}_4$ (γ - Fe_2O_3). The amorphous-like substance in the rust layer formed on mild steel possessed the structures of mainly α -FeOOH, showing superparamagnetism owing to its small particle size, and $\text{Fe}_{3-x}\text{O}_4$ (γ - Fe_2O_3), which were contained both in the inner and the outer rust layers.

The cross section of the rust layer is wavy and undulating, with thick and thin parts. Thus the thickness of the rust layer is quite uneven. According to Asami and Kikuchi^[44], the thin parts of the rust layer correspond to regions where a protective rust layer covers the steel, whereas the rust layer in the thick parts is less protective. These authors, in their interesting work on mild steel specimens exposed for 17 years under a bridge in a coastal industrial atmosphere, focus on differences between the composition of the thick and thin parts of the rust layer. Using TEM/ED they try to determine the proportion (semi-quantitative) of α -FeOOH, β -FeOOH, γ -FeOOH, Fe_3O_4 and amorphous rust in the rust layer cross section, as identified by ED patterns. As this technique cannot distinguish between maghemite and magnetite, the contribution of both was assigned to magnetite.

The main rust constituent was α -FeOOH, which appeared almost homogeneously throughout the rust layer. The chief difference between the thick and thin parts was the β -FeOOH and magnetite concentration; there being more β -FeOOH and less magnetite in the thick part of the rust layer. The formation of magnetite (or $\text{Fe}_{3-x}\text{O}_4$) and β -FeOOH is competitive, i.e. β -FeOOH is preferentially formed when there

are chloride ions. The average magnetite concentration in the rust layer is negatively correlated with the β -FeOOH concentration. Akaganeite is generally distributed in the surface region of the rust layer, probably due to the reaction between iron ions produced by corrosion and deposited atmospheric Cl^- ions. This species also appears in the inner layer due to Cl^- ions accidentally entering this region as water deposits containing chloride ions penetrate through cracks in the rust layer.

On the other hand, the thin rust part, where the main constituent is α -FeOOH and the β -FeOOH concentration is very low, has a protective nature because of the stabilised α -FeOOH and it is difficult for chloride ions to enter the rust layer.

The γ -FeOOH concentration and distribution bear no apparent relation with the type of steel, side of exposure or rust thickness. According to Yamashita *et al.*^[90], γ -FeOOH should exist on top of the α -FeOOH rust layer. However, it is not necessarily located in the upper part of the rust layer.

The location of amorphous rust is clear: near the boundary between the rust layer and the steel surface. Its concentration does not bear any relation with the thickness or the type of steel, but its quantification is difficult with the usual analytical techniques.

Dillmann *et al.*^[10], using a wide range of classic and advanced techniques (μ XRD, small angle X-ray scattering (SAXS), etc.), studied the composition, structure and porosity of ancient corrosion layers, finding:

(a) α -FeOOH has a fairly uniform distribution, occupying most of the rust layer thickness, and was in contact with the base metal.

(b) Although it presents the same optical appearance as goethite, γ -FeOOH is always confined to small zones in the outer part of the corrosion scale, often located along cracks.

(c) β -FeOOH is located in the outer part of the corrosion layer, sometimes along cracks. Akaganeite is also detected in the inner part of the corrosion products.

(d) No amorphous phases are clearly identified. This seems to be in contradiction with some authors, who have often found amorphous phases in the inner rust layer. According to Dillmann *et al.*^[10], the old age of the rust could explain the apparent absence of amorphous phases. This hypothesis is also shared by Yamashita *et al.*^[90], who suggests that during long exposure the amorphous inner layer may be transformed into a densely packed aggregate of goethite nanoparticles.

4.3. Prediction of corrosion rates

Mass loss measurements for mild steel in long-term exposure to different types of atmospheres show that it continues to corrode throughout the exposure time, irrespective of the test site location. The corrosion layers that form on mild steel are generally not very adherent or protective against further corrosion. This commonly results in the build-up of sheets of thick rust as the steel continues to corrode. These sheets eventually become detached and the exfoliated steel is newly exposed to the atmosphere^[84].

It is widely accepted that the long-term atmospheric corrosion of steel conforms to an equation of the form:

$$C = At^B \quad (21)$$

where C is metal loss, t is exposure time in years, and A and B are constants. According to Benarie and Lipfert^[91], equation (21) is a mass-balance equation showing that the diffusional process is rate-determining, and this rate depends on the diffusive properties of the layer separating the reactants.

The accuracy of equation (21) and its reliability to predict long-term corrosion have been demonstrated by Bohnenkamp *et al.*^[92], Legault and Preban^[93], Pourbaix^[94], Feliu and Morcillo^[95], and Benarie and Lipfert^[91], among others.

The exponential law, equation (21), with B close to 0.5, can result from an ideal diffusion-controlled mechanism when all the corrosion products remain on the metal surface. This situation seems to occur in slightly polluted inland atmospheres. On the other hand, B values of more than 0.5 arise due to acceleration of the diffusion process (e.g. as a result of rust detachment by erosion, dissolution, flaking, cracking, etc.). This situation is typical of marine atmospheres, even those with low chloride contents. Conversely, B values of less than 0.5 results from a decrease in the diffusion coefficient with time through recrystallisation, agglomeration, compaction, etc. of the rust layer.

In the special case when B = 1, the mean corrosion rate for one-year exposure is equal to A, the intersection of the line on the bilogarithmic plot with the abscissa t = 1 year. There is no physical sense in B > 1, as B = 1 is the limit for unimpeded diffusion (high permeable corrosion products or no layer at all). Values of B > 1 occur practically as exceptions, due, for instance, to outliers in the weight loss determinations. As a rule, B < 1.

Therefore, B could be used as an indicator for the physico-chemical behaviour of the corrosion

layer and hence for its interactions with the atmospheric environment. The value of B would thus depend both on the metal concerned, the local atmosphere, and the exposure conditions.

Some authors^[96 y 97], however, use a mixed linear-exponential equation, according to which a plot of corrosion against time would consist of an initial parabolic portion followed by a straight line.

In a previous paper, Morcillo *et al.*^[98] studied the goodness of the power model (Eq. (21)) on the basis of all the information compiled for mild steel in a comprehensive literature survey of corrosion data obtained in exposures of 10 years or more. It was decided to use this model rather than the power-linear model on account of its greater simplicity. In fact, only exponent B and corrosion after the first year of exposure, A, need to be known. The primary aim of that work was to determine B in terms of the type of atmosphere concerned.

As a conclusion of that study, the test stations were grouped according to the local atmosphere type, distinguishing rural-urban atmospheres and industrial atmospheres without any marine component from marine atmospheres. While exponent B varied greatly within each group, a trend was observed in these long-term tests for slopes of between 0.3 and 0.7 for rural, urban and industrial atmospheres and significantly greater (0.6 - 0.9) for marine atmospheres, whether or not they were close to the shoreline. This confirms the high significance of the marine atmosphere variable (which does not distinguish between chloride levels but refers exclusively to the marine character) in exponent B, as observed in a statistical study of Feliu *et al.*^[11]. The lower B is, the more protective the corrosion product layer on the metal surface.

Dean and Reiser^[99] reviewed the results obtained for steel in 8-year data from the ISOCORRAG collaborative programme^[11]. The time of wetness (TOW) positively affected the value of B for steel, i.e. a higher TOW causes the rust layer to be less protective. The other environmental effects (SO₂ and Cl⁻) did not appear to significantly affect the slope, although sulphation and salinity strongly affected the intercept (log A).

With regard to skyward-groundward values for steel, exponent B is higher on the groundward side, demonstrating the higher porosity there^[91].

5. FINAL CONSIDERATIONS

— This paper reviews the main theories and mechanisms of atmospheric corrosion appeared with time. Of particular importance to the

scientific knowledge are the researches of Stratmann and co-workers, showing for the first time that oxygen is reduced within the oxide layer and not at the metal / electrolyte interface.

- The present contribution pays special attention to two matters upon which relatively less information has been published: a) the morphology of steel corrosion product layers; and b) long term atmospheric corrosion. It seems to be a widespread view among researches on the dual layer structure of corrosion products formed on mild steel long-term exposed to atmosphere and the goodness of exponential law ($C = At^B$) to predict long-term atmospheric corrosion.

Acknowledgements

The authors would like to thank the Ministry of Science and Innovation for financial support (Project MAT 2008-06649). I. Díaz and H. Cano also acknowledge the PhD scholarship financed by CSIC-MICINN.

6. REFERENCES

- [1] S. W. Dean, D. Knotkova and K. Kresilova, *ISOCORRAG*, Internacional Atmospheric Exposure Program: Summary of Results, ASTM Data Series 71, ASTM International, West Conshohocken, 2010.
- [2] M. Morcillo, E. Almeida, B. Rosales, J. Uruchurtu and M. Marrocos, *Corrosión y Protección de Metales en las Atmósferas de Iberoamérica* (MICAT), CYTED, Madrid, 1998.
- [3] J. Tidblad, V. Kucera and A.A. Mikhailov, Report No 30, UN/ECE International Co-Operative Programme on Effects on Materials, Including Historic and Cultural Monuments (ICP Materials), 1998.
- [4] K. Barton, *Protection against Atmospheric Corrosion*, Eds. Wiley, London, 1976.
- [5] J. M. Costa, M. Morcillo and S. Feliu, *Effect of environmental parameters on atmospheric corrosion of metals*, In: *Air Pollution Control* (Vol. 2), P.N. Cheremisinoff (Ed.), Houston, EE.UU., 1989, pp. 197-238.
- [6] V. Kucera and E. Mattsson, *Atmospheric Corrosion*, In: *Corrosion Mechanisms*, F. Mansfeld (Ed.), New York, 1987, pp. 211-284.
- [7] C. Leygraf and T.E. Graedel, *Atmospheric Corrosion*, Wiley-Interscience, New York, 2000.
- [8] I. L. Rozenfeld, *Atmospheric Corrosion of Metals*, NACE, Houston, 1972.
- [9] S.W. Dean, *Corrosion-Prevention 9th-Proceedings*, Australasian Corrosion Association, Inc., November 28-30, Melbourne, Australia, 1994, pp. 1-12.
- [10] Ph. Dillmann, F. Mazaudier and S. Hoerlé, *Corros. Sci.* 46 (2004) 1.401-1.429.
- [11] S. Feliu, M. Morcillo and S. Feliu Jr., *Corros. Sci.* 34 (1993) 415-422.
- [12] C. Arroyave and M. Morcillo, *Trends in Corros. Res.* 2 (1997) 1-16.
- [13] R. M. Cornell and V. Schwertmann, *Iron Oxides in the Laboratory: Preparation and Characterization*, Wiley-VCH, Weinheim, 1991.
- [14] D.R. Lide, *CRC Handbook of Chemistry and Physics*, CRC Press, Boston, 1991.
- [15] W.F. Linke, *Solubilities of inorganic and metal-organic compounds*, Vol. 1, D. Van Nostrand Company, Princeton, 1958.
- [16] J.E. Hiller, *Werkst. Korros.* 17 (1966) 943-951.
- [17] T. Misawa, *Corros. Sci.* 13 (1973) 659-676.
- [18] E. Almeida, M. Morcillo, B. Rosales and M. Marrocos, *Mater. Corros.* 51 (2000) 859-864.
- [19] P. Keller, *Werkst. Korros.* 20 (1969) 102-108.
- [20] T. Misawa, T. Kyuno, W. Suëtaka and S. Shimodaira, *Corros. Sci.* 11 (1971) 35-48.
- [21] H. Schwarz, *Werkst. Korros.* 23 (1972) 648-663.
- [22] A.K. Singh, T. Ericsson and L. Häggström, *Corros. Sci.* 25 (1985) 931-945.
- [23] H. Baum, U. Rasemann, K. Rösler, S. Böhmer and E. Kunze, *Neue Hutte* 19 (1974) 423-429.
- [24] T. Misawa, K. Asami, K. Hashimoto and S. Shimodaira, *Corros. Sci.* 14 (1974) 279-289.
- [25] A. Raman and B. Kuban, *Corros.* 44 (1988) 483-488.
- [26] K. Rösler, H. Baum, O. Kukurs, A. Upite and D. Knotkova, *Prot. Met.* 17 (1981) 514-522.
- [27] R.A. Francis, *Proc. of the 10th Int. Congr. on Met. Corros.*, Vol. 1, Madras, India, November 28-30, Oxford and IBH Publishing Co., 1987, pp. 121-130.
- [28] T. Misawa, K. Hashimoto and S. Shimodaira, *Corros. Sci.* 14 (1974) 131-149.
- [29] K. Nomura, M. Tasaka and Y. Ujihira, *Corros.* 44 (1988) 131-135.
- [30] L. Espada, P. Merino, A. González and A. Sánchez, *Proc. of the 10th Int. Congr. on Met. Corros.*, Vol. 1, Oxford and IBH Publishing Co., Madras, India, 1987, pp. 3-7.
- [31] R.A. Antunes, J. Costa and D.L. Araujo, *Mater. Res.* 6 (2003) 403-408.
- [32] S. Oesch and P. Heimgartner, *Mater. Corros.* 47 (1996) 425-438.

- [33] S.E. Flores, Ph. Doctoral Thesis, Facultad de CC. Químicas, Universidad Complutense de Madrid, 1994.
- [34] S.E. Flores and M. Morcillo, *Surf. Coat. Int.*, 82 (1999) 19-25.
- [35] M. P. Cindra-Fonseca, I. N. Bastos, A. Caytuero and E. M. Baggio-Saitovitch. *Corros. Sci.* 49 (2007) 1.949-1.962.
- [36] D. de la Fuente, I. Díaz, J. Simancas, B. Chico and M. Morcillo, *Corros. Sci.* 53 (2011) 604-617.
- [37] A. Raman, S. Nasrazadani and L. Sharma, *Metallography* 22 (1989) 79-96.
- [38] A. Raman, S. Nasrazadani, L. Sharma and A. Razvan, *Prakt. Metallogr.* 24 (1987) 577-587.
- [39] A. Raman, S. Nasrazadani, L. Sharma and A. Razvan, *Prakt. Metallogr.* 24 (1987) 535-548.
- [40] A. Raman, A. Razvan, B. Kuban, K. A. Clement and E. Graves, *Corros.* 42 (1986) 447-455.
- [41] A. Razvan and A. Raman, *Prakt. Metallogr.* 23 (1986) 223-236.
- [42] K.K. Sagoe-Crentsil and F.P. Glasser, *Corros.* 49 (1993) 457-463.
- [43] M. Morcillo, I. Díaz, B. Chico, J. Simancas and D. de la Fuente, *Proc. of EUROCORR*, Moscow, Russia, September 13-17, 2010.
- [44] K. Asami and M. Kikuchi, *Corros. Sci.* 45 (2003) 2.671-2.688.
- [45] T. Kamimura, S. Nasu, T. Tazaki, K. Kuzushita and S. Morimoto, *Mater. Trans.* 43 (2002) 694-703.
- [46] H. Okada and H. Shimada, *Corros.* 30 (1974) 97-101.
- [47] E.S. Ayllón, S. L. Granese, C. Bonazzola and B. M. Rosales, *Rev. Iber. Corros. y Prot.* XVII, 3 (1986) 205-211.
- [48] W. H.J. Vernon, *Trans. Faraday Soc.* 31 (1935) 1.668-1.700.
- [49] G. Schikorr, *Werkst. Korros.* 14 (1963) 69-80.
- [50] U.R. Evans, *Trans. Inst. Met. Finish* 37 (1960) 1.
- [51] U.R. Evans and C.A.J. Taylor, *Corros. Sci.* 12 (1972) 227-246.
- [52] M. Stratmann, K. Bohnenkamp and H. J. Engell, *Corros. Sci.* 23 (1983) 969-985.
- [53] M. Stratmann and K. Hoffmann, *Corros. Sci.* 29 (1989) 1.329-1.352.
- [54] M. Stratmann and J. Müller, *Corros. Sci.* 36 (1994) 327-359.
- [55] M. Stratmann and H. Streckel, *Corros. Sci.* 30 (1990) 681-696.
- [56] M. Stratmann, H. Streckel, K.T. Kim and S. Crockett, *Corros. Sci.* 30 (1990) 715-734.
- [57] K. E. Heusler, *Z. Elektrochem.* 62 (1958) 582.
- [58] J. Bockris, D. Drazic and A. R. Despic, *Electrochim. Acta* 4 (1961) 325-361.
- [59] U.R. Evans, *Nature* 206 (1965) 980-982.
- [60] T. Nishimura, I. Tanaka and Y. Shimizu, *Tetsu-to-Hagane* 81 (1995) 1.079-1.084.
- [61] U.R. Evans, *Corros. Sci.* 9 (1969) 813-821.
- [62] H. Okada, Y. Hosoi and H. Naito, *Tetsu-To Hagane* 56 (1970) 277-284.
- [63] I. Matsushima and T. Ueno, *Boshoku Gijutsu* 17 (1968) 458-464.
- [64] H. Antony, L. Legrand, L. Maréchal, S. Perrin, Ph. Dillmann and A. Chaussé, *Electrochim. Acta* 51 (2005) 745-753.
- [65] I. Matsushima and T. Ueno, *Corros. Sci.* 11 (1971) 129-140.
- [66] H. Okada, Y. Hosoi and H. Naito, *Corros.* 26 (1970) 429-430.
- [67] I. Suzuki, N. Masuko and Y. Hisamatsu, *Corros. Sci.* 19 (1979) 521-535.
- [68] K. Barton and Z. Bartonova, *Werkst. Korros.* 20 (1969) 216-221.
- [69] M. Stratmann, K. Bohnenkamp and T. Ramchandran, *Corros. Sci.* 27 (1987) 905-926.
- [70] M. Stratmann, *Metal. Odlew.* 16 (1990) 46-52.
- [71] H. Schwarz, *Werkst. Korros.* 16 (1965) 93-103.
- [72] S. Feliu and M. Morcillo, *Corrosion atmosférica, In: Corrosion y Protección Metálicas*, S. Feliu and C. Andrade (Eds), CSIC, Nuevas Tendencias, Madrid, 1991, pp. 23-40.
- [73] G.M. Florianovitch, L.A. Sokolova and Y.A.M. Kolotykin, *Electrochim. Acta* 12 (1967) 879-887.
- [74] A.G. Tanner, *Chem. Ind.* 13 (1964) 1.027-1.028.
- [75] T.K. Ross and B. G. Callaghan, *Corros. Sci.* 6 (1966) 337-343.
- [75] J.F. Henriksen, *Corros. Sci.* 9 (1969) 573-577.
- [76] I. M. Allam, J. S. Arlow and H. Saricimen, *Corros. Sci.* 32 (1991) 417-432.
- [77] F. Corvo, *Corros.* 40 (1984) 170-175.
- [78] R. Ericsson, *Werkst. Korros.* 29 (1978) 400-403.
- [79] E. Almeida, M. Morcillo and B. Rosales, *Mater. Corros.* 51 (2000) 865-874.
- [80] ISO 9223, Corrosion of Metals and Alloys - Classification of Corrosivity of Atmospheres, ISO, Geneva, 1990.
- [81] D. Neff, L. Bellot-Gurlet, Ph. Dillmann, S. Reguer and L. Legrand, *J. Raman Spectrosc.* 37 (2006) 1.228-1.237.
- [82] S.J. Oh, D.C. Cook and H. E. Townsend, *Corros. Sci.* 41 (1999) 1.687-1.702.
- [83] D.C. Cook, *Corros. Sci.* 47 (2005) 2550-2570.
- [84] M. Yamashita, K. Asami, T. Ishikawa, T. Ohtsuka, H. Tamura and T. Misawa, *Zairyo-to Kankyo* 50 (2001) 521-530.
- [85] J. Simancas, K.L. Scrivener and M. Morcillo, *A Study of rust morphology, contamination and*

- porosity by backscattered electron imaging, In: *Atmospheric Corrosion*. W. W. Kirk, H. H. Lawson (Eds.), ASTM STP 1239, Philadelphia, 1995.
- [86] G.B. Clark, G. K. Berukshtis and Z. I. Ignatova, *Proc. of the 3rd Int. Congr. on Met. Corros.*, Moscow, Rusia, 1969, pp. 406-412.
- [87] I. Suzuki, Y. Hisamatsu and N. Masuko, *J. electrochem. Soc.* 127 (1980) 2.210-2.215.
- [88] H. Okada, Y. Osoi, K. Yukawa and H. Naito, *Proc. of the 4th Int. Congr. on Met. Corros.*, Amsterdam, The Netherlands, 1969, pp. 392-398.
- [89] M. Yamashita, H. Miyuki, Y. Matsuda, H. Nagano and T. Misawa, *Corros. Sci.* 36 (1994) 283-299.
- [90] M. Benarie and F.L. Lipfert, *Atmos. Environ.* 20 (1986) 1947-1958.
- [91] K. Bohnenkamp, G. Burgmann and W. Schwenk, *Stahl Eisen* 93 (1973) 1045-1060.
- [92] R. A. Legault and G. Preban, *Corros.* 31 (1975) 117-122.
- [93] M. Pourbaix, *The linear bilogarithmic law for atmospheric corrosion*, In: *Atmospheric Corrosion*, W. H. Aylor, (Ed.), J. Wiley and Sons, New York, 1982, pp. 107-121.
- [94] S. Feliu and M. Morcillo, *Atmospheric corrosion testing in Spain*, In: *Atmospheric Corrosion*, W. H. Aylor, (Ed.), J. Wiley and Sons, New York, 1982, pp. 913-922.
- [95] D. Knotkova, K. Barton and M. Cerny, *Atmospheric corrosion testing in Czechoslovakia*, In: *Atmospheric Corrosion*, W. H. Aylor, (Ed.), J. Wiley and Sons, New York, 1982, pp. 991-1014.
- [96] Y.N. Mikhailovski, P.V. Strekalov and V.V. Agafonov, *Zaschita Metallov* 16 (1980) 396-413.
- [97] M. Morcillo, J. Simancas and S. Feliu, *Long-term atmospheric corrosion in Spain: results after 13 to 16 years of exposure and comparison with worldwide data*. In: *Atmospheric Corrosion*, W.W. Kirk, H.H. Lawson (Eds.), ASTM STP 1239, Philadelphia, 1995, pp. 195-214.
- [98] S.W. Dean and D.B. Reiser, *Analysis of long-term atmospheric corrosion results from ISO-CORRAG Program*. In: *Outdoor Atmospheric Corrosion*, H. E. Townsend (Ed.), ASTM STP 1421, Philadelphia, 2002.